

# Comparison of resonant inelastic x-ray scattering spectra and dielectric loss functions in copper oxides

Jungho Kim, D. S. Ellis, H. Zhang, and Young-June Kim\*  
*Department of Physics, University of Toronto, Toronto, Ontario, Canada M5S 1A7*

J. P. Hill  
*Department of Condensed Matter Physics and Materials Science, Brookhaven National Laboratory, Upton, New York 11973, USA*

F. C. Chou†  
*Center for Materials Science and Engineering, MIT, Cambridge, Massachusetts 02139, USA*

T. Gog and D. Casa  
*XOR, Advanced Photon Source, Argonne National Laboratory, Argonne, Illinois 60439, USA*  
 (Received 27 December 2008; revised manuscript received 4 February 2009; published 30 March 2009)

We report empirical comparisons of Cu *K*-edge indirect resonant inelastic x-ray scattering (RIXS) spectra, taken at the Brillouin-zone center, with optical dielectric loss functions measured in a number of copper oxides. The RIXS data are obtained for Bi<sub>2</sub>CuO<sub>4</sub>, CuGeO<sub>3</sub>, Sr<sub>2</sub>Cu<sub>3</sub>O<sub>4</sub>Cl<sub>2</sub>, La<sub>2</sub>CuO<sub>4</sub>, and Sr<sub>2</sub>CuO<sub>2</sub>Cl<sub>2</sub>, and analyzed by considering both incident and scattered-photon resonances. An incident-energy-independent response function is then extracted. The dielectric loss functions, measured with spectroscopic ellipsometry, agree well with this RIXS response, especially in Bi<sub>2</sub>CuO<sub>4</sub> and CuGeO<sub>3</sub>.

DOI: [10.1103/PhysRevB.79.094525](https://doi.org/10.1103/PhysRevB.79.094525)

PACS number(s): 74.25.Gz, 74.72.-h, 78.20.-e, 78.70.Ck

## I. INTRODUCTION

Since the pioneering study of NiO by Kao *et al.*,<sup>1</sup> indirect resonant inelastic x-ray scattering (RIXS) (Refs. 2 and 3) in the hard x-ray regime has been regarded as a promising momentum-resolved spectroscopic tool for investigating charge excitations in solids.<sup>4–6</sup> A variety of systems, including nickelates,<sup>7,8</sup> manganites,<sup>9,10</sup> and cuprates,<sup>11–19</sup> have been studied by *K*-edge RIXS, revealing new and interesting charge excitations. Despite these early experiments, further developments of this promising technique have been hindered by the lack of a systematic theoretical understanding. The RIXS cross section is complicated because the resonant contribution generally involves correlation between more than two particles.<sup>2,5,20</sup> To date, theoretical studies of the RIXS cross section have mostly been limited to model-dependent calculations.<sup>21–24</sup> This is in contrast with the cross section for nonresonant inelastic x-ray scattering (IXS) which measures the two-particle charge correlation function.<sup>25</sup>

In this context, recent theoretical studies by Ament and co-workers<sup>2,3</sup> are noteworthy. Working in the limits of a local, strong (or weak), and short-lived core-hole potential, they were able to show that, in these limits, the RIXS cross section can be factored into a resonant prefactor that depends on the incident and scattered-photon energies and the dynamic structure factor,  $S(\mathbf{q}, \omega)$ .<sup>3</sup> This result has important implications for the interpretation of RIXS spectra since this approach then suggests that with proper handling of the prefactor, RIXS can be considered as a weak probe that measures  $S(\mathbf{q}, \omega)$ . It is therefore important to test whether this theory can be applied to real systems or not, and delineate any necessary conditions for the applicability of Ref. 3.

There have been previous attempts to empirically relate the RIXS cross section to a calculable two-particle correla-

tion function.<sup>10,11,14,26</sup> Direct comparisons of the RIXS spectra and calculated  $S(\mathbf{q}, \omega)$  have been made for SrCuO<sub>2</sub> (Ref. 14) and Nd<sub>0.5</sub>Sr<sub>0.5</sub>MnO<sub>3</sub>.<sup>10</sup> In Ref. 26, a purely empirical comparison between the RIXS spectra and  $S(\mathbf{q}, \omega)$  measured with electron energy loss spectroscopy (EELS) has been made for a number of copper oxides. However, these comparisons are made with the RIXS spectra obtained with a particular incident photon energy, and thus are limited in their scope. Abbamonte and co-workers<sup>11</sup> were able to show that by taking into account the incident and scattered-photon energy resonance, the RIXS spectra of La<sub>2</sub>CuO<sub>4</sub> could be described by a single spectral function. They also argued that the so-obtained response function is related to  $S(\mathbf{q}, \omega)$ , without explicit comparison. Therefore, it is apparent that a quantitative empirical comparison, taking into account the incident-energy dependence, is necessary to address the issue regarding the RIXS response function.

In this paper, we report a systematic comparison of the RIXS spectra and the dielectric loss functions in various copper oxides: Bi<sub>2</sub>CuO<sub>4</sub>, CuGeO<sub>3</sub>, Sr<sub>2</sub>Cu<sub>3</sub>O<sub>4</sub>Cl<sub>2</sub>, La<sub>2</sub>CuO<sub>4</sub>, and Sr<sub>2</sub>CuO<sub>2</sub>Cl<sub>2</sub>. We measured the RIXS spectrum of each sample at the  $\Gamma$  position and extracted a response function that does not depend on the incident energy. This response function is compared with the optical dielectric loss function, measured using spectroscopic ellipsometry on the same sample. Dielectric loss-function data from published EELS studies are also used to augment the optical data. We show that overall energy loss dependence of the RIXS response function is in good agreement with the optical dielectric loss function over a wide energy range for all samples. In particular, the agreement is excellent for the local systems Bi<sub>2</sub>CuO<sub>4</sub> and CuGeO<sub>3</sub>, suggesting that the RIXS response is intimately related to the dynamic structure factor and thus to the charge density-density correlation function in these materi-

TABLE I. Summary of the RIXS experimental conditions and fitting parameters for the samples studied.  $\omega_{\text{res}}$  and  $\Gamma$  are the scattered-photon resonance energy and the damping due to finite lifetime of intermediate states, respectively, and  $|U|$  is the local core-hole potential. Each  $Q$  position, denoted in reciprocal-lattice unit, corresponds to either 2D or one-dimensional (1D) zone center. The  $z$  direction in the case of polarization refers to the direction perpendicular to the copper oxygen plaquette.

Sample	$Q$ (rlu)	Polarization	$\omega_{\text{res}}$ (eV)	$\Gamma$ (eV)	$ U $ (eV)	$T$ (K)
Bi <sub>2</sub> CuO <sub>4</sub>	(0,0,3)	$\epsilon \perp z$	8993.7	3.2	5.7	20
CuGeO <sub>3</sub>	(1.5,0,0)	$\epsilon \sim \ z$ <sup>a</sup>	8985.7	2.5	4.3	300
Sr <sub>2</sub> Cu <sub>3</sub> O <sub>4</sub> Cl <sub>2</sub>	(0,0,9)	$\epsilon \perp z$	8989.0	3.5	4.5	300
La <sub>2</sub> CuO <sub>4</sub>	(3,0,0)	$\epsilon \  z$	8989.3	2.5	2.5	20
Sr <sub>2</sub> CuO <sub>2</sub> Cl <sub>2</sub>	(0,0,11)	$\epsilon \perp z$	8992.4	3.0	2.6	300

<sup>a</sup>The polarization was along the crystallographic  $b$  direction.

als. On the other hand, additional low-energy spectral features are observed for the corner-sharing two-dimensional (2D) copper oxides such as La<sub>2</sub>CuO<sub>4</sub> and Sr<sub>2</sub>CuO<sub>2</sub>Cl<sub>2</sub>, indicating that nonlocal nature of intermediate states may play an important role in such compounds.

## II. EXPERIMENTAL DETAILS

The Cu  $K$ -edge RIXS experiments were carried out at the 9IDB beamline at the Advanced Photon Source. Channel-cut Si(444)/Si(333) monochromators, various detector slits, and a diced Ge(733) analyzer with 1 m radius of curvature were utilized. The data shown here are obtained with low resolution [full width at half maximum (FWHM) of the elastic line: 300–400 meV] unless otherwise specified. The single-crystal samples of Bi<sub>2</sub>CuO<sub>4</sub>, CuGeO<sub>3</sub>, and La<sub>2</sub>CuO<sub>4</sub> were grown using the traveling solvent floating zone method, while the Sr<sub>2</sub>Cu<sub>3</sub>O<sub>4</sub>Cl<sub>2</sub> and Sr<sub>2</sub>CuO<sub>2</sub>Cl<sub>2</sub> single crystals were prepared using the CuO flux method. The experimental conditions for each measurement are summarized in Table I. All RIXS measurements were carried out at the appropriate  $\mathbf{q}=0$  reciprocal space positions. We have also studied the optical properties of the same samples with spectroscopic ellipsometry using a variable angle spectroscopic ellipsometer (VASE, Woollam). The energy dependence (1–6.2 eV) of real and imaginary parts of the dielectric function has been obtained at room temperature. The spectra shown here are obtained with the photon polarization parallel to the copper oxygen plaquette.

## III. EXPERIMENTAL RESULTS

From Eq. (26) in Ref. 3, the RIXS intensity  $I(\omega, \omega_i)$  at  $\mathbf{q}=0$  can be written as<sup>27</sup>

$$I \sim P(\omega, \omega_i) S(\omega) \delta(\omega - \omega_s + \omega_i), \quad (1)$$

where  $\omega_i$  and  $\omega_s$  are the incident and scattered-photon energies, respectively, and  $\omega = \omega_i - \omega_s$  is the energy loss. Here,  $S(\omega) \equiv S(\mathbf{q}=\mathbf{0}, \omega)$  is the density response function at  $\mathbf{q}=\mathbf{0}$ .<sup>5,11</sup> Note that the resonance behavior involving

intermediate states is all contained in the prefactor  $P(\omega, \omega_i) = [(\omega_s - \omega_{\text{res}})^2 + \Gamma^2]^{-1} [(\omega_i - \omega_{\text{res}} - |U|)^2 + \Gamma^2]^{-1}$ , which consists of two Lorentzian functions with damping ( $\Gamma$ ) due to the finite lifetime of intermediate states. Each of these Lorentzian functions represent resonant behavior of incident and scattered photons, resonating at  $\omega_{\text{res}} + |U|$  and  $\omega_{\text{res}}$ , respectively, where  $|U|$  is the local core-hole potential.

We have analyzed our data by fitting all scans using Eq. (1), leaving  $\omega_{\text{res}}$ ,  $\Gamma$ , and the overall amplitude as free parameters. The fitting parameters for each sample are listed in Table I. Note that the peak position of the  $K$ -edge x-ray absorption spectrum ( $\omega_{\text{XAS}}$ ) is taken to be the incident photon resonance energy  $\omega_{\text{res}} + |U|$ . Since the incident photon energy  $\omega_i$  is fixed for each scan, the  $[(\omega_i - \omega_{\text{XAS}})^2 + \Gamma^2]^{-1}$  factor becomes a constant for each scan, leaving a single Lorentzian function in the prefactor. This remaining Lorentzian function centered at  $\omega_{\text{res}}$  with width  $\Gamma$  describes the scattered-photon resonance, which is necessary to obtain satisfactory fits.<sup>28</sup>

In order to illustrate the use of the scattered-photon resonance, the RIXS spectra of CuGeO<sub>3</sub> obtained with four different incident energies are plotted as a function of  $\omega_s$  in Fig. 1(a). For each scan, there are two strong energy-loss features centered at  $\omega=3.8$  eV and 6.5 eV. Although the energy-loss positions of these features do not change from scan to scan, the ratio between these two features varies quite a lot. The  $\omega=6.5$  eV peak is strongest when  $\omega_i=8992$  eV, while the  $\omega=3.8$  eV peak is strongest when  $\omega_i=8990$  eV. These observations seem to suggest that the energy loss is a material-specific property arising from  $S(\omega)$ , while the intensity variation is due to the resonance prefactor. The scattered-photon resonant prefactor, shown as the Lorentzian envelope function in Fig. 1(a), describes the intensity ratio variation between these two peaks very well. In other words, by fitting all our data to Eq. (1), it is possible to extract an  $\omega_i$ -independent part of the spectrum:  $S(\omega)$ .

Similar analysis of the  $\omega_i$  and  $\omega_s$  dependences of the spectra has also been carried out for the other samples. The data for La<sub>2</sub>CuO<sub>4</sub> are shown in Figs. 1(c) and 1(d). Again the envelope function seems to describe the intensity variation as a function of  $\omega_i$  well. In Figs. 2(a)–2(e), the resulting  $S(\omega)$  spectra are shown as a function of  $\omega$ . The elastic tail in the RIXS raw data are fitted to a Lorentzian function and subtracted in this plot. We find that, for a given material, the spectra obtained with different incident energies collapse onto a single spectrum that represents  $S(\omega)$ , as expected. We note that a similar analysis was carried out in Refs. 11, 33, and 34, but with the assumption that the incident and scattered intermediate states were degenerate ( $U=0$ ) (Refs. 11 and 33) or nearly degenerate ( $|U|=1$  eV).<sup>34</sup> One could take the same approach here, but we found that assuming two distinct intermediate states for  $\omega_i$  and  $\omega_s$  is essential in describing all the spectral features simultaneously. As discussed in Ref. 3, these two resonances come from the intermediate-state energies separated by the core-hole potential. Table I lists the values of  $\omega_{\text{res}}$  obtained from our fitting and  $|U| = \omega_{\text{XAS}} - \omega_{\text{res}}$ .

Next, we compare the extracted  $S(\omega)$  with the measured optical response functions. One of the key results in Ref. 3 is that apart from the prefactor, the RIXS should measure  $S(\omega)$ ,

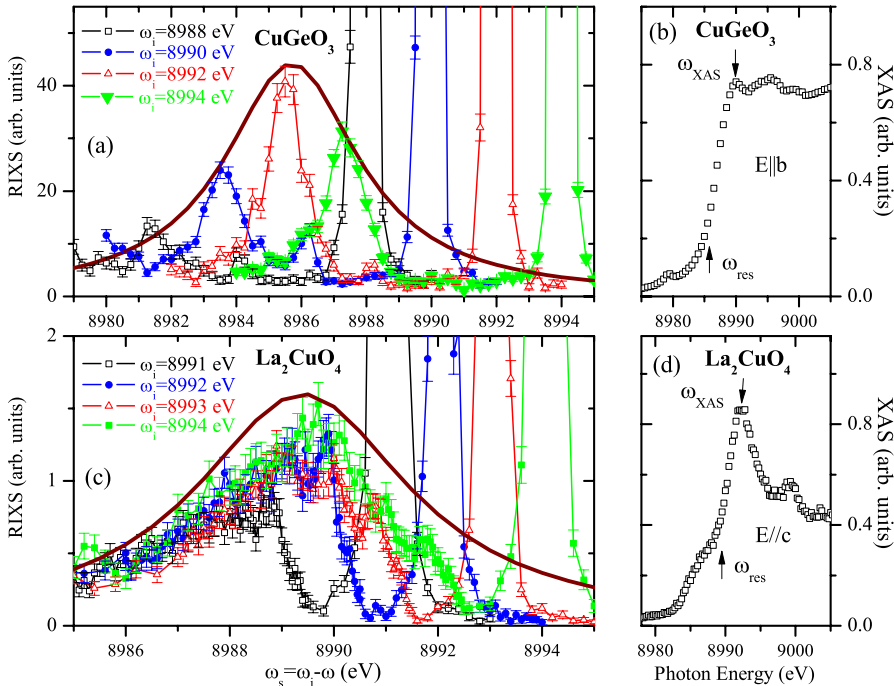


FIG. 1. (Color online) (a) The  $K$ -edge RIXS spectra taken with four incident photon energies as a function of the scattered-photon energy ( $\omega_s$ ) for CuGeO<sub>3</sub>. Note that the inelastic intensity follows an envelope function (solid line), indicating the scattered-photon resonance. (b) The total fluorescence yield obtained near the Cu  $K$ -edge for CuGeO<sub>3</sub>. Two resonance energies,  $\omega_{\text{XAS}}$  and  $\omega_{\text{res}}$ , are noted. Similar plots for La<sub>2</sub>CuO<sub>4</sub> are shown in (c) and (d). The RIXS data for La<sub>2</sub>CuO<sub>4</sub> are taken from Ref. 13.

which captures the physics of the valence electron system. Several studies have also argued that the response function of RIXS corresponds to the dynamic structure factor,  $S(\mathbf{q}, \omega)$ , or equivalently the dielectric loss-function,  $\text{Im}[-1/\epsilon(\omega)]$ .<sup>2,3,10,11,14,26</sup> Having obtained an incident-energy-independent RIXS response function, we are now in a position to test this idea directly. To do so, we obtained optical spectra from ellipsometry measurements on the same samples used in the RIXS experiments. As a first comparison, we plot both the imaginary part of complex dielectric function,  $\epsilon_2(\omega)$ , and  $\text{Im}[-1/\epsilon(\omega)]$  in Fig. 2(a). It is clear that  $S(\omega)$  is most similar to  $\text{Im}[-1/\epsilon(\omega)]$ , but not to  $\epsilon_2(\omega)$ . In Fig. 2, measured  $\text{Im}[-1/\epsilon(\omega)]$  spectra for the other systems are overlaid with the  $S(\omega)$  spectra. We also include the available EELS spectra near  $\mathbf{q}=0$  from the literature.<sup>29–32</sup> It is well known that EELS at  $\mathbf{q}=0$  also measures  $\text{Im}[-1/\epsilon(\omega)]$ . Note that the RIXS data are plotted using an arbitrary vertical scaling in making these comparison.

Figure 2 shows that the extracted  $S(\omega)$  is in good overall agreement with the general shape of  $\text{Im}[-1/\epsilon(\omega)]$  for all five systems studied, regardless of the detailed characteristics of the particular charge excitations. In particular, Bi<sub>2</sub>CuO<sub>4</sub> and CuGeO<sub>3</sub> show excellent agreement in terms of the number of peaks and their positions. In the other systems, however, it is not easy to see a one-to-one correspondence with particular features, in part because the spectra themselves are more complex with several features in the low-energy region. These will be discussed in more detail later. Nevertheless, as indicated by the arrows in Figs. 2(c)–2(e), the position of the insulating gap and the increase in  $S(\omega)$  above 7–8 eV agree reasonably well for the two data sets.

To make a detailed comparison for La<sub>2</sub>CuO<sub>4</sub> and Sr<sub>2</sub>CuO<sub>2</sub>Cl<sub>2</sub>, we plot high-resolution ( $\sim 130$  meV) RIXS data and ellipsometry data for these two materials in Fig. 3 focusing on the low-energy region. The high-resolution  $S(\omega)$  is obtained via the same procedure as described above, with

the same parameters. Features labeled A and C in the two RIXS spectra correspond to the lowest-energy charge excitations, and presumably have the same origin as the charge gap in  $\text{Im}[-1/\epsilon(\omega)]$ , yet their spectral shape appears different for the two techniques. We also observe an additional peak, B, around 3 eV, in La<sub>2</sub>CuO<sub>4</sub>, which is not apparent in the ellipsometry data. Similarly, feature D in Sr<sub>2</sub>CuO<sub>2</sub>Cl<sub>2</sub> is not observed in the ellipsometry, while strong features are observed between C and D. In the case of La<sub>2</sub>CuO<sub>4</sub>,  $S(\omega)$  has a small peak below A which is due to a  $d$ - $d$  excitation.<sup>35</sup> The  $d$ - $d$  excitation also shows up in ellipsometry data, though its spectral weight is suppressed.

#### IV. DISCUSSION AND SUMMARY

In order to understand the observed discrepancy, it is useful to consider the structural differences between the cuprate samples studied here. Although the main structural building block in all these samples is a plaquette composed of one Cu and four oxygen atoms, the network formed by these CuO<sub>4</sub> plaquettes is very different, as shown in Fig. 2 insets. In Bi<sub>2</sub>CuO<sub>4</sub>, these plaquettes are isolated, while they form an edge-sharing chain in CuGeO<sub>3</sub>. On the other hand, the plaquettes form a two-dimensional corner-sharing network in the other three compounds. It is important to realize that the interaction between the valence electron system and the  $1s$  core hole in the intermediate state is *nonlocal* in the case of such corner-sharing copper oxides due to the 180° Cu-O-Cu bond in these compounds.<sup>36,37</sup> Therefore, one can imagine that the local core-hole potential approximation used in Ref. 3 may break down in this case. The importance of nonlocality can also be inferred from the cluster calculation,<sup>38</sup> in which a cluster substantially larger than the plaquette was necessary to explain the observed XAS spectrum in La<sub>2</sub>CuO<sub>4</sub>. Such nonlocal valence electron states (commonly referred to as Zhang-Rice singlet states)<sup>39</sup> in corner-sharing

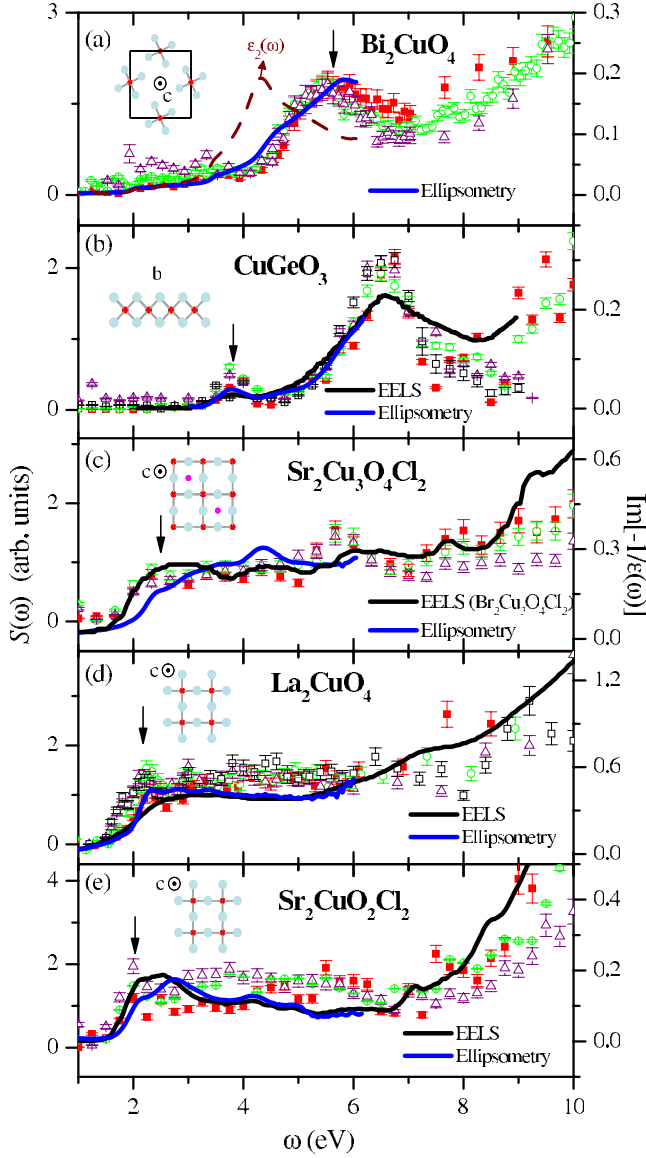


FIG. 2. (Color online) Comparison of  $S(\omega)$  with the measured  $\text{Im}[-1/\epsilon(\omega)]$  for various cuprates. Different symbols are used to denote RIXS spectra obtained with different incident energies. These incident photon energies (in eV) are (a) 8997.5 (■), 8998.5 (○), 8999.5 (△); (b) 8988 (■), 8990 (○), 8992 (△), 8994 (□); (c) 8992 (■), 8993 (○), 8994 (△); (d) 8991 (■), 8992 (○), 8993 (△), 8994 (□); and (e) 8993 (■), 8994 (○), 8995 (△). The EELS data for  $\text{CuGeO}_3$ ,  $\text{La}_2\text{CuO}_4$ , and  $\text{Sr}_2\text{CuO}_2\text{Cl}_2$  are taken from Refs. 29–31, respectively. Although there is no EELS spectrum for  $\text{Sr}_2\text{Cu}_3\text{O}_4\text{Cl}_2$  available in the literature, that of  $\text{Ba}_2\text{Cu}_3\text{O}_4\text{Cl}_2$  is shown (Ref. 32).

copper oxides are probably responsible for screening the core-hole potential, effectively lowering its value.<sup>40</sup> In fact, the values of  $|U|$  reported in Table I for  $\text{La}_2\text{CuO}_4$  and  $\text{Sr}_2\text{CuO}_2\text{Cl}_2$  are much smaller than those for other compounds.

We note that in their study of  $\text{HgBa}_2\text{CuO}_{4+\delta}$ , Lu *et al.*<sup>18</sup> reported that RIXS reveals more excitations than conventional two-particle spectroscopy such as optical spectroscopy. In addition, RIXS experiments on  $\text{La}_2\text{CuO}_4$  have

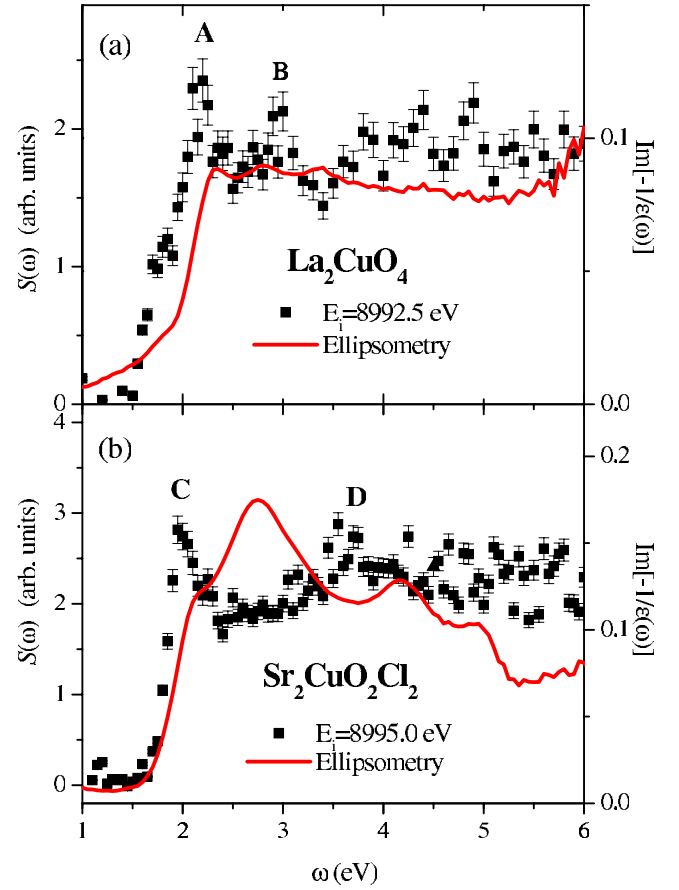


FIG. 3. (Color online) The function  $S(\omega)$  extracted from high-resolution RIXS data and compared with  $\text{Im}[-1/\epsilon(\omega)]$  for (a)  $\text{La}_2\text{CuO}_4$  and (b)  $\text{Sr}_2\text{CuO}_2\text{Cl}_2$ .

shown that there are many charge excitation peaks in addition to the lowest 2 eV peak.<sup>7,13,35</sup> The observed fine structure, such as the features B and D in Fig. 3, thus could arise from the difference in the matrix elements that enhances certain spectral features selectively.

In summary, we show that overall spectral features of the *indirect* resonant inelastic x-ray scattering response function are in a reasonable agreement with the optical dielectric loss function over a wide energy range. In the case of  $\text{Bi}_2\text{CuO}_4$  and  $\text{CuGeO}_3$ , we observe that the incident-energy-independent response function,  $S(\mathbf{q}=\mathbf{0}, \omega)$ , matches very well with the dielectric loss function,  $\text{Im}[-1/\epsilon(\omega)]$ , suggesting that the local core-hole approximation treatment of Ref. 3 works well in these compounds. We also find that corner-sharing two-dimensional copper oxides exhibit more complex excitation features than those observed in the dielectric loss functions. Our study seems to suggest that one can probe two-particle charge correlation function with indirect resonant inelastic x-ray scattering.

#### ACKNOWLEDGMENTS

We would like to thank Luuk Ament, Fiona Forte, and J. van den Brink for the discussions. Research at the University



of Toronto was supported by the NSERC of Canada, Canadian Foundation for Innovation, and Ontario Ministry of Research and Innovation. Work at Brookhaven was supported by the U.S. DOE, Office of Science under Contract No. DE-

AC02-98CH10886. Use of the Advanced Photon Source was supported by the U.S. DOE, Office of Science, Office of Basic Energy Sciences, under Contract No. W-31-109-ENG-38.

\*yjkim@physics.utoronto.ca

†Present address: Center for Condensed Matter Sciences, National Taiwan University, Taipei 10717, Taiwan.

- <sup>1</sup>C. C. Kao, W. A. L. Caliebe, J. B. Hastings, and J. M. Gillet, *Phys. Rev. B* **54**, 16361 (1996).
- <sup>2</sup>J. van den Brink and M. A. van Veenendaal, *Europhys. Lett.* **73**, 121 (2006).
- <sup>3</sup>L. J. P. Ament, F. Forte, and J. van den Brink, *Phys. Rev. B* **75**, 115118 (2007).
- <sup>4</sup>A. Kotani and S. Shin, *Rev. Mod. Phys.* **73**, 203 (2001).
- <sup>5</sup>P. M. Platzman and E. D. Isaacs, *Phys. Rev. B* **57**, 11107 (1998).
- <sup>6</sup>J. P. Hill, C. C. Kao, W. A. L. Caliebe, M. Matsubara, A. Kotani, J. L. Peng, and R. L. Greene, *Phys. Rev. Lett.* **80**, 4967 (1998).
- <sup>7</sup>E. Collart, A. Shukla, J.-P. Rueff, P. Leininger, H. Ishii, I. Jarriège, Y. Q. Cai, S.-W. Cheong, and G. Dhalenne, *Phys. Rev. Lett.* **96**, 157004 (2006).
- <sup>8</sup>S. Wakimoto, H. Kimura, K. Ishii, K. Ikeuchi, T. Adachi, M. Fujita, K. Kakurai, Y. Koike, J. Mizuki, Y. Noda, A. Said, Y. Shvydko, and K. Yamada, arXiv:0806.3302 (unpublished).
- <sup>9</sup>T. Inami, T. Fukuda, J. Mizuki, S. Ishihara, H. Kondo, H. Nakao, T. Matsumura, K. Hirota, Y. Murakami, S. Maekawa, and Y. Endoh, *Phys. Rev. B* **67**, 045108 (2003).
- <sup>10</sup>S. Grenier *et al.*, *Phys. Rev. Lett.* **94**, 047203 (2005).
- <sup>11</sup>P. Abbamonte, C. A. Burns, E. D. Isaacs, P. M. Platzman, L. L. Miller, S. W. Cheong, and M. V. Klein, *Phys. Rev. Lett.* **83**, 860 (1999).
- <sup>12</sup>M. Z. Hasan, E. D. Isaacs, Z. X. Shen, L. L. Miller, K. Tsutsui, T. Tohyama, and S. Maekawa, *Science* **288**, 1811 (2000).
- <sup>13</sup>Y. J. Kim, J. P. Hill, C. A. Burns, S. Wakimoto, R. J. Birgeneau, D. Casa, T. Gog, and C. T. Venkataraman, *Phys. Rev. Lett.* **89**, 177003 (2002).
- <sup>14</sup>Y. J. Kim *et al.*, *Phys. Rev. Lett.* **92**, 137402 (2004).
- <sup>15</sup>K. Ishii *et al.*, *Phys. Rev. Lett.* **94**, 187002 (2005).
- <sup>16</sup>K. Ishii *et al.*, *Phys. Rev. Lett.* **94**, 207003 (2005).
- <sup>17</sup>S. Suga, S. Imada, A. Higashiya, A. Shigemoto, S. Kasai, M. Sing, H. Fujiwara, A. Sekiyama, A. Yamasaki, C. Kim, T. Nomura, J. Igarashi, M. Yabashi, and T. Ishikawa, *Phys. Rev. B* **72**, 081101(R) (2005).
- <sup>18</sup>L. Lu *et al.*, *Phys. Rev. Lett.* **95**, 217003 (2005).
- <sup>19</sup>J. P. Hill *et al.*, *Phys. Rev. Lett.* **100**, 097001 (2008).
- <sup>20</sup>T. P. Devereaux and R. Hackl, *Rev. Mod. Phys.* **79**, 175 (2007).
- <sup>21</sup>K. Tsutsui, T. Tohyama, and S. Maekawa, *Phys. Rev. Lett.* **83**, 3705 (1999).
- <sup>22</sup>T. Nomura and J. I. Igarashi, *Phys. Rev. B* **71**, 035110 (2005).
- <sup>23</sup>R. S. Markiewicz and A. Bansil, *Phys. Rev. Lett.* **96**, 107005 (2006).
- <sup>24</sup>F. Vernay, B. Moritz, I. S. Elfimov, J. Geck, D. Hawthorn, T. P. Devereaux, and G. A. Sawatzky, *Phys. Rev. B* **77**, 104519 (2008).
- <sup>25</sup>P. M. Platzman and P. A. Wolf, *Waves and Interactions in Solid State Plasmas* (Academic, New York, 1973).
- <sup>26</sup>Y.-J. Kim, J. P. Hill, S. Wakimoto, R. J. Birgeneau, F. C. Chou, N. Motoyama, K. M. Kojima, S. Uchida, D. Casa, and T. Gog, *Phys. Rev. B* **76**, 155116 (2007).
- <sup>27</sup>We use the spinless fermion expression from Ref. 3 since double occupancy can be ignored in these copper oxide compounds due to the strong on-site Coulomb interaction. Note also that the energy notation used here is slightly different from that of Ref. 3.
- <sup>28</sup>We made the self-absorption correction for  $\omega_s$  following the approach in L. Tröger *et al.*, *Phys. Rev. B* **46**, 3283 (1992). We found that this correction has a negligible effect within our statistics and energy resolution.
- <sup>29</sup>S. Atzkern, M. Knupfer, M. S. Golden, J. Fink, A. Hübsch, C. Waidacher, K. W. Becker, W. von der Linden, M. Weiden, and C. Geibel, *Phys. Rev. B* **64**, 075112 (2001).
- <sup>30</sup>M. Terauchi and M. Tanaka, *Micron* **30**, 371 (1999).
- <sup>31</sup>A. S. Moskvina, R. Neudert, M. Knupfer, J. Fink, and R. Hayn, *Phys. Rev. B* **65**, 180512(R) (2002).
- <sup>32</sup>O. Knauff, T. Boske, M. Knupfer, M. S. Golden, G. Krabbes, and J. Fink, *J. Low Temp. Phys.* **105**, 353 (1996).
- <sup>33</sup>G. Döring, C. Sternemann, A. Kaprolat, A. Mattila, K. Hamalainen, and W. Schulke, *Phys. Rev. B* **70**, 085115 (2004).
- <sup>34</sup>L. Lu, J. N. Hancock, G. Chabot-Couture, K. Ishii, O. P. Vajk, G. Yu, J. Mizuki, D. Casa, T. Gog, and M. Greven, *Phys. Rev. B* **74**, 224509 (2006).
- <sup>35</sup>D. S. Ellis, J. P. Hill, S. Wakimoto, R. J. Birgeneau, D. Casa, T. Gog, and Y.-J. Kim, *Phys. Rev. B* **77**, 060501(R) (2008).
- <sup>36</sup>M. A. van Veenendaal, H. Eskes, and G. A. Sawatzky, *Phys. Rev. B* **47**, 11462 (1993).
- <sup>37</sup>K. Okada and A. Kotani, *Phys. Rev. B* **52**, 4794 (1995).
- <sup>38</sup>C. Li, M. Pompa, A. C. Castellano, S. D. Longa, and A. Bianconi, *Physica C* **175**, 369 (1991).
- <sup>39</sup>F. C. Zhang and T. M. Rice, *Phys. Rev. B* **37**, 3759 (1988).
- <sup>40</sup>T. Böske, K. Maiti, O. Knauff, K. Ruck, M. S. Golden, G. Krabbes, J. Fink, T. Osafune, N. Motoyama, H. Eisaki, and S. Uchida, *Phys. Rev. B* **57**, 138 (1998).